ЖЭТФ, 2021, том 159, вып. 4, стр. 711–718

NICKELATE SUPERCONDUCTORS: AN ONGOING DIALOG BETWEEN THEORY AND EXPERIMENTS

A. S. Botana [a], ***F. Bernardini*** [b], ***A. Cano*** [c*]

[a] *Department of Physics, Arizona State University*
Tempe, AZ 85287, USA

[b] *Dipartimento di Fisica, Università di Cagliari*
IT-09042, Monserrato, Italy

[c] *Université Grenoble Alpes, CNRS, Grenoble INP, Institut Néel*
38042, Grenoble, France

Received December 4, 2020,
revised version December 4, 2020
Accepted for publication December 5, 2020

Contribution for the JETP special issue in honor of I. E. Dzyaloshinskii's 90th birthday

DOI: 10.31857/S0044451021040131

Unconventional superconductivity, understood as superconductivity beyond the electron-phonon paradigm, remains a defining problem in condensed matter [1]. The challenge is exemplified by the high-T_c cuprates, and nickelates joined the club last year after Hwang and collaborators reported superconductivity in Sr-doped $NdNiO_2$ thin films [2]. Here, we provide an overview on nickelate superconductors.

Experimental facts. Rare-earth infinite-layer nickelates RNiO$_2$ have been known for decades [3–6]. This special type of nickelates can be seen as the $n = \infty$ members of the series $R_{n+1}Ni_nO_{2n+2}$, with each member containing n-NiO$_2$ planes (see Fig. 1, R — rare-earth). The synthesis of these materials is typically achieved by first growing the nickelate in its RNiO$_3$ perovskite version, and then removing the apical oxygens from the NiO$_6$ octahedra with reducing agents such as hydrogen [7]. This is the so-called topotactic reduction which, in practice, may have unwanted consequences such as hydrogen intercalation into the sample [8]. Superconductivity in RNiO$_2$ (R = Pr, Nd) emerges via charge carrier doping as in the cuprates. This has only been achieved by means of thin-film growth techniques [9], while superconductivity in doped bulk samples is yet to be reported [10–12].

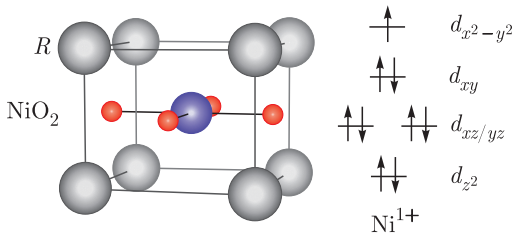

Fig. 1. Ball-and-stick model of the unit cell of the infinite-layer nickelates RNiO$_2$ and sketch of the formal $3d^9$ electronic configuration of a Ni^{1+} atom in square-planar coordination. The set of d orbitals is frequently divided into the subsets e_g-like $= \{d_{x^2-y^2}, d_{z^2}\}$ and t_{2g}-like $= \{d_{xy}, d_{xz}, d_{yz}\}$ as in octahedral coordination

Figure 2 shows the temperature-composition phase diagram of Sr-doped $NdNiO_2$ and $PrNiO_2$ [13,14]. The measured resistivity as a function of temperature shows metallic behavior, with a low-temperature upturn systematically observed (Fig. 2). This upturn can be attributed to weak localization, or it could be reminiscent of Kondo physics [15]. These systems can be seen as weak insulators or bad metals all along the phase diagram, in marked contrast to cuprates. Besides, no signature of long-range magnetic order has been reported so far for the parent infinite-layer nickelates [4, 5, 16]. However, a recent NMR study has pointed out the presence of antiferromagnetic fluctuations and quasi-static antiferromagnetic order below 40 K in $Nd_{0.85}Sr_{0.15}NiO_2$ [17].

* E-mail: andres.cano@neel.cnrs.fr

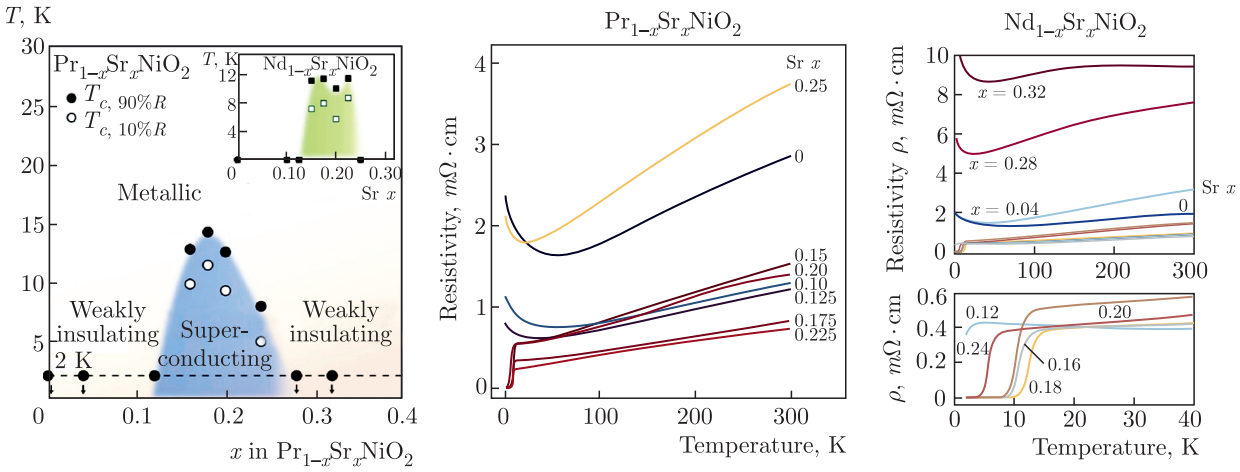

Fig. 2. Temperature vs composition phase diagram of the superconducting infinite-layer nickelates reported so far — i. e. Sr-doped $NdNiO_2$ and $PrNiO_2$ thin films on $SrTiO_3$ substrates — and corresponding resistivity data (from [13] and [14]). Sr-doping is equivalent to hole doping in these systems. The superconducting T_c reaches 15 K in the best superconducting samples. The resistivity in the normal state shows metallic behavior as a function of temperature, with a Kondo-like upturn systematically observed for both underdoped and overdoped samples. The metallicity is however rather poor, and hence these systems can be seen as bad metals with weakly insulating features. At the same time, enhanced metallicity has been repeatedly reported in superconducting samples when compared to the non-superconducting ones

The transport data reported so far is still sample dependent, with nominally equivalent samples displaying finite resistivity or a complete drop [13, 18, 19]. Also, whether the original $LaNiO_2$ reference compound hosts superconductivity or not remains an important open question. This difference may be "simply" due to sample quality and/or the presence of topotactic hydrogen in $LaNiO_2$ — i. e. the formation of $LaNiO_2H$ instead of $LaNiO_2$ [8]. Otherwise, it may be more intrinsically related to the rare-earth elements themselves — i. e. closed vs open $4f$ shells and the corresponding magnetic moments.

Figure 3 illustrates the measured Hall coefficient for $RNiO_2$ that has been observed to change sign both as a function of temperature and as a function of doping. This evidences an underlying multiband character in infinite-layer nickelates, which is another important fundamental difference when compared to cuprates. Such a multiband picture has been confirmed by X-ray spectroscopic techniques [20–22]. However, in contrast to the Hall data, the changes in the X-ray spectra observed as a function of Sr-doping have been interpreted in terms of doped holes residing in the Ni-$3d_{x^2-y^2}$ orbitals without necessarily invoking multiband effects [21].

The single particle tunneling spectrum has been measured on (Nd,Sr)NiO_2 [23]. The spectrum was found to be inhomogenous, with different features at different locations of the sample. One of the predominant features correspond to a V-shape spectrum. However, features corresponding to a full s-wave gap are equally observed and, in some cases, even a mixture of the two.

Theoretical considerations.

Single-particle picture. At the single-particle DFT level, the calculations support the multiband picture of the infinite-layer nickelates in agreement with experimental data [20, 24–34]. These calculations reveal a large Fermi-surface sheet due to Ni-$3d_{x^2-y^2}$ holes akin to that in cuprates (see Fig. 4). However, the Fermi surface displays additional electron pockets due to $5d$ states associated to the rare-earth $5d$ states ($5d_{z^2}$ at Γ and $5d_{xy}$ at A). This can be seen as a self-doping effect promoted by the hybridization of these formally empty states with the Ni-$3d$ bands. This effect is totally absent in the cuprates. Moreover, the Ni-$3d_{z^2}$ states turn out to be partially occupied and additionally hybridized with the R-$5d$ ones. Thus, the full e_g-like $= \{d_{x^2-y^2}, d_{z^2}\}$ sector of the Ni-$3d$ states becomes "active" in infinite-layer nickelates. In part, this results from the comparatively large difference in on-site energies promoting charge from O-$2p$ to Ni-$3d$ orbitals, i. e. the so-called charge-transfer energy ~ 4 eV.

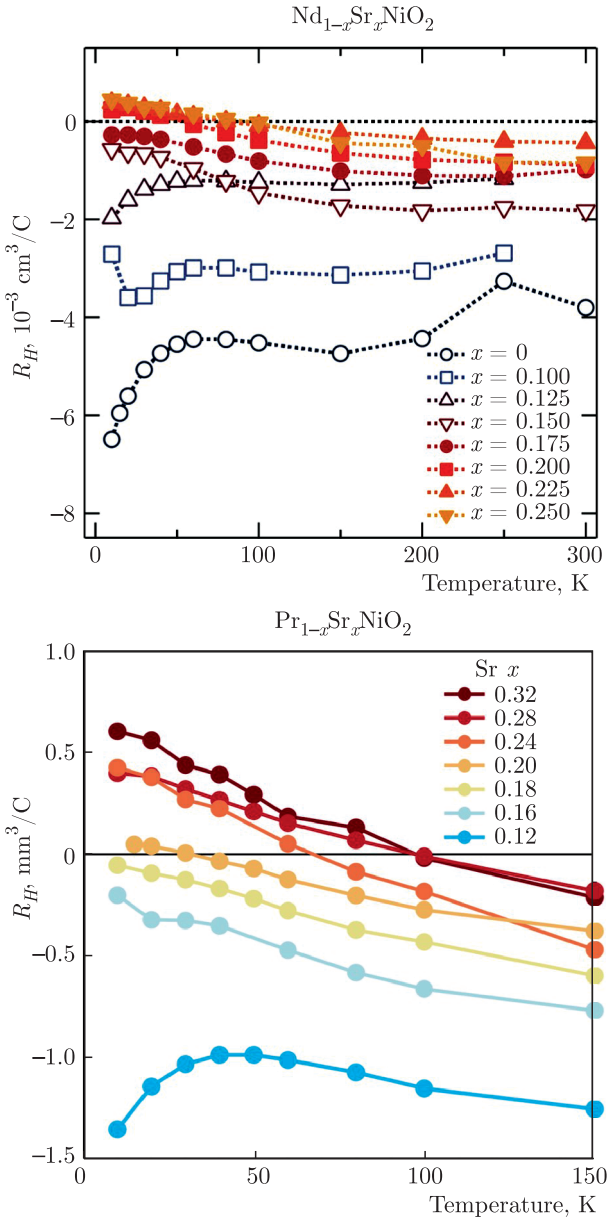

Fig. 3. Hall coefficient R_H measured in $NdNiO_2$ and $PrNiO_2$ as a function of temperature and Sr doping [13, 14]. In both cases, the Hall coefficient below 100 K changes sign as a function of Sr content (x in $R_{1-x}Sr_xNiO_2$). The main charge carriers have electron character in the parent compounds ($x = 0$), which eventually changes to holes upon increasing doping. This was the first experimental hint of an underlying multiband picture

Many-body correlation effects: Cooper pairing. The standard electron-phonon mechanism has been ruled out as the main reason for superconductivity in infinite-layer nickelates [28]. Instead, repulsive interactions mediated by spin-fluctuations were right away argued to drive the Cooper pairing in these systems [26, 27, 36, 37]. Specifically, d-wave superconductivity was concluded from complementary random phase approximation (RPA) and fluctuation exchange (FLEX) calculations for many-body multi-orbital Hamiltonians in which the non-interacting part maps the relevant DFT bands. More recently, these results have been confirmed using advanced techniques in which the starting vertex is non-perturbative so that the local correlations are fully included [38].

The same conclusion about the d-wave symmetry of the superconducting gap was reached in [27] from a standard t–J model constructed in a similar way for the Ni-$3d_{x^2-y^2}$ states. Further, the specific self-doping features of the nickelates have inspired an extended t–J model that generically addresses the strong-coupling limit of similar multiband systems [39]. Alternatively, if the Hund's coupling J between $d_{x^2-y^2}$ and d_{z^2} Ni orbitals plays a dominant role, it has been pointed out that the Cooper pairing can be interpreted within a spin-freezing scenario as due to local-moment fluctuations, rather than to pure antiferromagnetic fluctuations [40].

Many-body correlation effects: Electronic structure. The DFT picture has been revised using many-body perturbation theory at the *GW* level, thus treating correlations *ab initio* [41, 42]. The low-energy physics remains essentially unaffected, with only small changes obtained in the interacting Fermi surface and in the quasiparticle spectral weights near the Fermi level. The Ni-$3d_{x^2-y^2}$ bandwidth reduces slightly while the Ni-$3d_{z^2}$ one increases as the O-$2p$ states are further shifted to lower energies (1.5 eV further down from the Fermi level) [41]. The latter, however, represents a rather substantial change, and hence suggests that the canonical charge-transfer-insulator picture is even more unlikely for the infinite-layer nickelates in the *GW* framework. These changes are also tied to an important shift of the empty $4f$ states [41], which should be taken as a warning regarding their role in the overall physics of these materials.

DFT+DMFT (dynamical mean-field theory) calculations according to Hubbard–Hund interaction Hamiltonians have been performed to further scrutinize the correlated nature of the different orbitals and clarify the multiband nature in $RNiO_2$ [15, 35, 38, 40, 43–51]. In addition, DMFT has also been applied in combination with the quasiparticle self-consistent *GW* approximation in a parameter-free fashion [42, 52]. The overall multiband picture remains robust and the re-

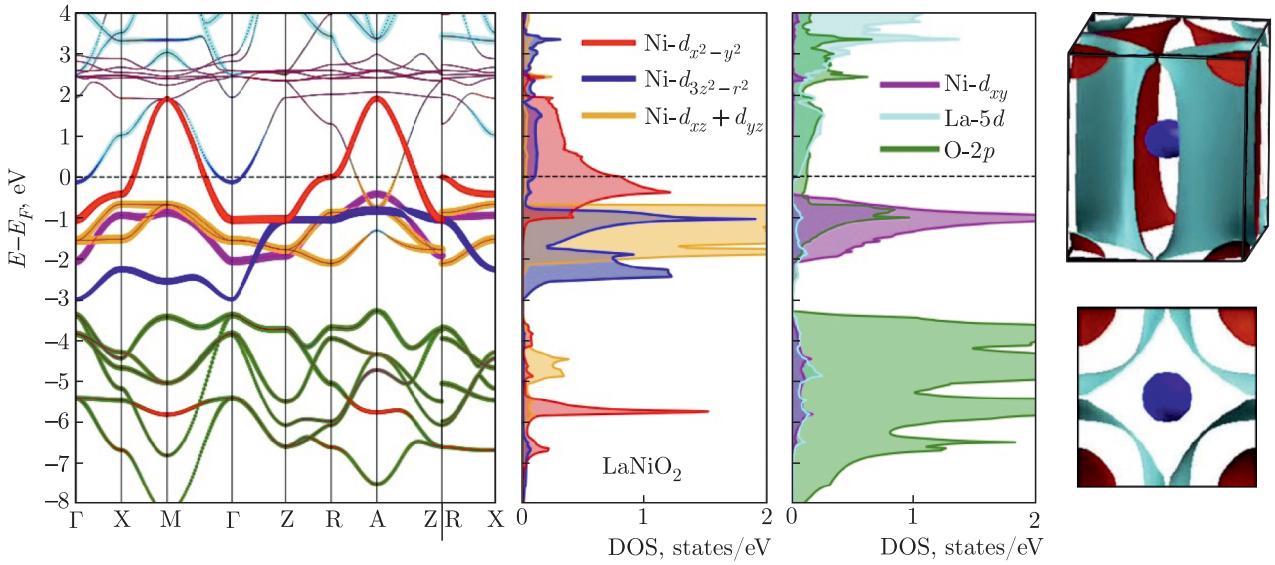

Fig. 4. Electronic structure of the reference material $LaNiO_2$ obtained at the DFT level (fat-band plot, density of states (DOS) and Fermi surface from [25] and [35]). In addition to the main Ni-$3d_{x^2-y^2}$ cuprate-like band crossing the Fermi level, the Ni-$3d_{z^2}$ states are not completely occupied in these systems. Further, the system has a multiband character due to La-$5d$ states that give rise to additional electron pockets and "self-dope" the Ni-$3d_{x^2-y^2}$ hole-like Fermi surface. The O-$2p$ states, in turn, are comparatively far below the Fermi level

sults confirm the above trends. However, the effective mass renormalization or inverse quasiparticle weight $m^*/m = 1/Z$ undergoes substantial orbital-selective changes [35, 44, 46]. The Ni-$d_{x^2-y^2}$ band is found to have a tendency towards localization such that a Mott gap can eventually open if the Hubbard interaction is large enough [44, 45]. The R-$5d$ self-doping bands, in contrast, remain much more weakly correlated [44, 45]. Beyond that, the DMFT results define an apparent Hubbard vs Hund dichotomy in which the multiband aspects of infinite-layer nickelates are emphasized differently [53].

Magnetism. A magnetic ground state is consistently obtained in theoretical studies [20, 24, 25, 48, 49, 53–57]. In DFT+DMFT a near degeneracy of spin orders is obtained that implies magnetic frustration especially upon doping [48, 49]. This frustration arises due to the involvement of both $3d_{x^2-y^2}$ and $3d_{z^2}$ Ni orbitals and may be responsible for the experimental suppression of long-range magnetic order. A complementary point of view is obtained via DFT calculations, as the antiferromagnetic ground state portrays a one-dimensional-like van Hove singularity of d_{z^2} character pinned at the Fermi level [58]. This singularity makes the antiferromagnetic phase eventually unstable to spin-density disproportionation, breathing and half-breathing lattice distortions, and charge-density disproportionation. A different point of view suggests that $5d$ conduction electrons could screen the Ni spins, suppressing magnetism and giving rise to a Kondo effect like that seen in heavy fermion materials [15]. Beyond that, an intrinsic difference that could be behind the differing properties across the RNiO$_2$ series, notably the emergence of superconductivity itself, is the presence/absence of magnetic rare-earth elements [33, 59].

Interfacial and surface effects. The local electronic properties of the infinite-layer nickelate thin films were first addressed in [60] and shortly after in [61]. The epitaxial growth of the RNiO$_2$/SrTiO$_3$ heterostructures can in principle yield different atomic boundaries between the sample and the substrate [60]. The most obvious configuration corresponds to a fully reduced nickelate having its ($RO\rightarrow$) R layer directly on top of the TiO$_2$-terminated substrate. This configuration, however, was found to be energetically unstable, which is a local-scale manifestation of the thermodynamic fragility of these phases. Thus, the infinite-layer nickelate prefers to face a RO layer to the substrate, and the same conclusion holds even for a direct-growth

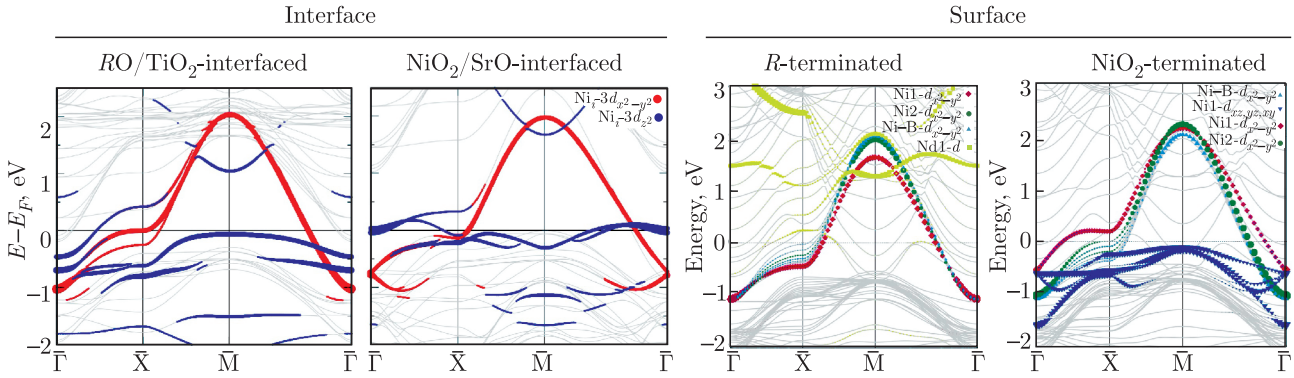

Fig. 5. Electronic band structure of the infinite-layer nickelates at the $R\mathrm{NiO_2}/\mathrm{SrTiO_3}$ interface (left) and at the surface (right) for different atomic configurations (the colors highlight the main contributions of the interfacial/surface Ni-3d states near the Fermi level; adapted from [60] and [62]). In both cases the nature of the self-doping effect — obtained from the R-5d states in the bulk — changes or even disappears depending on the local atomic configuration. At the same time, other Ni-3d states are pushed closer to the Fermi level and locally supplement the system with flat band features

process. This "chemical" reconstruction was further shown to produce drastic changes in the electronic structure at the interface [60]. The interfacial chemical reconstruction according to the $R \to \mathrm{Sr} \to RO \to \mathrm{SrO}$ sequence is to some extent equivalent to localized hole doping. This local doping was found to deplete the self-doping R-5d states at the interface. Specifically, the R-5d states are first replaced by Ti-3d ones, which are then pushed above the Fermi level for the SrO configuration (see Fig. 5). At the same time, the intefacial Ni-3d_{z^2} states are driven closer to the Fermi energy so that they manifestly participate in the low-energy physics. Thus, the Kondo-lattice features are expected to be fundamentally different at the interfaces where, in addition, the Ni-e_g sector will likely be fully active. Besides, this sector is supplemented by a markedly flat band character of the interfacial Ni-3d_{z^2} states, so that interface-specific correlation effects may be promoted [60].

This picture was subsequently confirmed for thin films with asymmetric boundaries [61, 63, 64]. In that case, the different polar discontinuities yield an effective built-in electric field across the film and polar layers can be formed at the surface and at the interface [63]. These layers show antiparallel NiO_2 displacements, but otherwise are decoupled. At the interface with the substrate, a two-dimensional electron gas extending over several layers together with the aforementioned depletion of the self-doping R-5d states is obtained [61, 63]. In addition, the combined effect of magnetism (G-AFM order) and correlations has been considered at the DFT+U level [63]. This enhances the itineracy of the Ni-3d_{z^2} orbitals at the interface with the substrate, while the magnetism is essentially suppressed at the surface to vacuum. Further, the effect of the nickelate termination anticipated in [60] is specifically considered in relation to superconductivity in [62]. Thus, it is argued that the d-wave superconducting gap expected for the bulk may transform into a $s_{\pm}$-wave one at the NiO_2-terminated surface, and it is also suggested that a surface $s + id$-wave state may be realized under the appropriate conditions.

Conclusions and perspectives. The recent discovery of superconductivity in infinite-layer nickelates has created intense excitement. These systems have been rapidly scrutinized from many different angles, using a battery of experimental and theoretical tools. The initial motivation of drawing analogies with the high-T_c cuprates has thus been surpassed. Instead, the accumulated results have now consolidated these systems as a new class of unconventional superconducting materials.

Specifically, the rare-earth infinite-layer nickelates have been confirmed to host a distinct multiband interplay, on top of which electronic correlations build and determine the main properties of these systems. This interplay is present already within the Ni sector itself, as not only the Ni-3$d_{x^2-y^2}$ states but also the Ni-3d_{z^2} ones are found to be active. This further introduces specific correlation effects and the bad metallic, or weakly insulating behavior is now understood as a

direct manifestation of these correlations. However, a Hubbard vs Hund dichotomy has emerged that is yet to be clarified. In addition, the rare-earth states introduce extra specific ingredients such as the self-doping effect and a $4f$-ness that may qualitatively be even more important. When it comes to the central question, that is, the emergence of superconductivity in these materials, it has been ascribed to spin fluctuations (in a broad sense), and there is now experimental evidence of incipient antiferromagnetic order.

Additional progress to further clarify these aspects, as well as the actual superconducting properties beyond T_c can be naturally expected [65]. In this context, it is fundamental to determine whether the lack of superconductivity in the $LaNiO_2$ reference material is intrinsic and also why thin films are superconducting while bulk samples are not.

More importantly, a crucial issue to address is: is there a whole new family of nickel-based unconventional superconductors waiting to be discovered? This question currently motivates the experimental and computational search of new alternative materials [66–74]. Other layered nickelates are obtained via oxygen reduction from the corresponding Ruddlesden–Popper phases [75,76]. The $n = 2$ and 3 materials, in particular, have been known for a while and, similarly to the $n = \infty$ ones, have also been discussed as candidate superconductors [66–71, 77]. Recently, La-based $n = 4$–6 parent Ruddlesden–Popper phases have also been synthesized [78]. Reduction of these compounds is particularly promising as they would realize d-electron counts that can be directly mapped into the dome area of filling. In addition, current epitaxial growth techniques can be exploited as an alternative route to engineer Ni-based heterostructures mimicking the $R_{n+1}Ni_nO_{2n+2}$ series with the advantage of better sample quality and doping control [60]. The infinite-layer case itself has proven to be a challenging but successful example in this respect.

Shedding light on these issues will not only help understanding superconductivity in these specific low-valence layered nickelates but will also provide new perspectives about the nature of unconventional superconductivity in general.

Acknowledgments. We dedicate this review on this 1-year-old topic to I. E. Dzyaloshinskii in celebration of his 90th birthday. We thank M. R. Norman and X. Blase for useful comments.

Funding. A. B. acknowledges the support from NSF DMR 2045826.

The full text of this paper is published in the English version of JETP.

REFERENCES

1. M. R. Norman, Science **332**, 196 (2011).

2. D. Li, K. Lee, B. Y. Wang, M. Osada, S. Crossley, H. R. Lee, Y. Cui, Y. Hikita, and H. Y. Hwang, Nature (London) **572**, 624 (2019).

3. M. Crespin, P. Levitz, and L. Gatineau, J. Chem. Soc., Faraday Trans. 2 **79**, 1181 (1983).

4. M. Hayward, M. Green, M. Rosseinsky, and J. Sloan, J. Amer. Chem. Soc. **121**, 8843 (1999).

5. M. Hayward and M. Rosseinsky, Sol. St. Sci. **5**, 839 (2003).

6. M. Crespin, O. Isnard, F. Dubois, J. Choisnet, and P. Odier, J. Sol. St. Chem. France **178**, 1326 (2005).

7. A. Ikeda, T. Manabe, and M. Naito, Physica C **506**, 83 (2014).

8. L. Si, W. Xiao, J. Kaufmann, J. M. Tomczak, Y. Lu, Z. Zhong, and K. Held, Phys. Rev. Lett. **124**, 166402 (2020).

9. K. Lee, B. H. Goodge, D. Li, M. Osada, B. Y. Wang, Y. Cui, L. F. Kourkoutis, and H. Y. Hwang, APL Mater. **8**, 041107 (2020).

10. Q. Li, C. He, J. Si, X. Zhu, Y. Zhang, and H.-H. Wen, Commun. Mater. **1**, 16 (2020).

11. B.-X. Wang, H. Zheng, E. Krivyakina, O. Chmaissem, P. P. Lopes, J. W. Lynn, L. C. Gallington, Y. Ren, S. Rosenkranz, J. F. Mitchell, and D. Phelan, Phys. Rev. Mater. **4**, 084409 (2020).

12. C. He, X. Ming, Q. Li, X. Zhu, J. Si, and H.-H. Wen, arXiv:2010.11777.

13. D. Li, B. Y. Wang, K. Lee, S. P. Harvey, M. Osada, B. H. Goodge, L. F. Kourkoutis, and H. Y. Hwang, Phys. Rev. Lett. **125**, 027001 (2020).

14. M. Osada, B. Y. Wang, K. Lee, D. Li, and H. Y. Hwang, arXiv:2010.16101.

15. G.-M. Zhang, Y.-F. Yang, and F.-C. Zhang, Phys. Rev. B **101**, 020501 (2020).

16. A. Ikeda, Y. Krockenberger, H. Irie, M. Naito, and H. Yamamoto, Appl. Phys. Express **9**, 061101 (2016).

17. Y. Cui, C. Li, Q. Li, X. Zhu, Z. Hu, Y.-F. Yang, J. S. Zhang, R. Yu, H.-H. Wen, and W. Yu, arXiv: 2011.09610.

18. S. Zeng, C. S. Tang, X. Yin, C. Li, M. Li, Z. Huang, J. Hu, W. Liu, G. J. Omar, H. Jani, Z. S. Lim, K. Han, D. Wan, P. Yang, S. J. Pennycook, A. T. S. Wee, and A. Ariando, Phys. Rev. Lett. **125**, 147003 (2020).

19. M. Osada, B. Y. Wang, B. H. Goodge, K. Lee, H. Yoon, K. Sakuma, D. Li, M. Miura, L. F. Kourkoutis, and H. Y. Hwang, Nano Lett. **20**, 5735 (2020).

20. M. Hepting, D. Li, C. J. Jia, H. Lu, E. Paris, Y. Tseng, X. Feng, M. Osada, E. Been, Y. Hikita, Y. D. Chuang, Z. Hussain, K. J. Zhou, A. Nag, M. Garcia-Fernandez, M. Rossi, H. Y. Huang, D. J. Huang, Z. X. Shen, T. Schmitt, H. Y. Hwang, B. Moritz, J. Zaanen, T. P. Devereaux, and W. S. Lee, Nature Mater. **19**, 381 (2020).

21. M. Rossi, H. Lu, A. Nag, D. Li, M. Osada, K. Lee, B. Y. Wang, S. Agrestini, M. Garcia-Fernandez, Y. D. Chuang, Z. X. Shen, H. Y. Hwang, B. Moritz, K.-J. Zhou, T. P. Devereaux, and W. S. Lee, arXiv:2011.00595.

22. B. H. Goodge, D. Li, M. Osada, B. Y. Wang, K. Lee, G. A. Sawatzky, H. Y. Hwang, and L. F. Kourkoutis, arXiv:2005.02847.

23. Q. Gu, Y. Li, S. Wan, H. Li, W. Guo, H. Yang, Q. Li, X. Zhu, X. Pan, Y. Nie, and H.-H. Wen, arXiv:2006.13123.

24. K.-W. Lee and W. E. Pickett, Phys. Rev. B **70**, 165109 (2004).

25. A. S. Botana and M. R. Norman, Phys. Rev. X **10**, 011024 (2020).

26. H. Sakakibara, H. Usui, K. Suzuki, T. Kotani, H. Aoki, and K. Kuroki, Phys. Rev. Lett. **125**, 077003 (2020).

27. X. Wu, D. Di Sante, T. Schwemmer, W. Hanke, H. Y. Hwang, S. Raghu, and R. Thomale, Phys. Rev. B **101**, 060504 (2020).

28. Y. Nomura, M. Hirayama, T. Tadano, Y. Yoshimoto, K. Nakamura, and R. Arita, Phys. Rev. B **100**, 205138 (2019).

29. J. Gao, S. Peng, Z. Wang, C. Fang, and H. Weng, Nat. Sci. Rev. (2020), https://doi.org/10.1093/nsr/nwaa218, nwaa218.

30. P. Jiang, L. Si, Z. Liao, and Z. Zhong, Phys. Rev. B **100**, 201106 (2019).

31. E. Been, W.-S. Lee, H. Y. Hwang, Y. Cui, J. Zaanen, T. Devereaux, B. Moritz, and C. Jia, arXiv:2002.12300.

32. F. Bernardini, V. Olevano, and A. Cano, Phys. Rev. Res. **2**, 013219 (2020).

33. J. Kapeghian and A. S. Botana, Phys. Rev. B **102**, 205130 (2020).

34. J. Krishna, H. LaBollita, A. O. Fumega, V. Pardo, and A. S. Botana, Phys. Rev. B **102**, 224506 (2020).

35. Y. Wang, C.-J. Kang, H. Miao, and G. Kotliar, Phys. Rev. B **102**, 161118 (2020).

36. T. Zhou, Y. Gao, and Z. Wang, Sci. China Phys. Mech. Astron. **63**, 287412 (2020).

37. P. Adhikary, S. Bandyopadhyay, T. Das, I. Dasgupta, and T. Saha-Dasgupta, Phys. Rev. B **102**, 100501 (2020).

38. M. Kitatani, L. Si, O. Janson, R. Arita, Z. Zhong, and K. Held, npj Quant. Mater. **5**, 59 (2020).

39. Y.-H. Zhang and A. Vishwanath, Phys. Rev. Res. **2**, 023112 (2020).

40. P. Werner and S. Hoshino, Phys. Rev. B **101**, 041104 (2020).

41. V. Olevano, F. Bernardini, X. Blase, and A. Cano, Phys. Rev. B **101**, 161102 (2020).

42. F. Petocchi, V. Christiansson, F. Nilsson, F. Aryasetiawan, and P. Werner, arXiv:2006.00394.

43. S. Ryee, H. Yoon, T. J. Kim, M. Y. Jeong, and M. J. Han, Phys. Rev. B **101**, 064513 (2020).

44. F. Lechermann, Phys. Rev. B **101**, 081110 (2020).

45. J. Karp, A. S. Botana, M. R. Norman, H. Park, M. Zingl, and A. Millis, Phys. Rev. X **10**, 021061 (2020).

46. I. Leonov, S. L. Skornyakov, and S. Y. Savrasov, Phys. Rev. B **101**, 241108 (2020).

47. F. Lechermann, Phys. Rev. X **10**, 041002 (2020).

48. I. Leonov and S. Y. Savrasov, arXiv:2006.05295.

49. X. Wan, V. Ivanov, G. Resta, I. Leonov, and S. Y. Savrasov, arXiv:2008.07465.

50. C.-J. Kang and G. Kotliar, arXiv:2007.15383.

51. Z.-J. Lang, R. Jiang, and W. Ku, arXiv:2005.00022.

52. B. Kang, C. Melnick, P. Semon, G. Kotliar, and S. Choi, arXiv:2007.14610.

53. F. Lechermann, arXiv:2012.09796.

54. H. Zhang, L. Jin, S. Wang, B. Xi, X. Shi, F. Ye, and J.-W. Mei, Phys. Rev. Res. **2**, 013214 (2020).

55. Y. Gu, S. Zhu, X. Wang, J. Hu, and H. Chen, Commun. Phys. **3**, 84 (2020).

56. Z. Liu, Z. Ren, W. Zhu, Z. Wang, and J. Yang, npj Quant. Mater. **5**, 31 (2020).

57. A. S. Botana and V. Pardo, arXiv:2012.02711.

58. M.-Y. Choi, K.-W. Lee, and W. E. Pickett, Phys. Rev. Res. **2**, 033445 (2020).

59. M.-Y. Choi, K.-W. Lee, and W. E. Pickett, Phys. Rev. B **101**, 020503 (2020).

60. F. Bernardini and A. Cano, J. Phys. Mater. **3**, 03LT01 (2020).

61. B. Geisler and R. Pentcheva, Phys. Rev. B **102**, 020502 (2020).

62. X. Wu, K. Jiang, D. Di Sante, W. Hanke, A. P. Schnyder, J. Hu, and R. Thomale, arXiv:2008.06009.

63. Y. Zhang, L.-F. Lin, W. Hu, A. Moreo, S. Dong, and E. Dagotto, Phys. Rev. B **102**, 195117 (2020).

64. R. He, P. Jiang, Y. Lu, Y. Song, M. Chen, M. Jin, L. Shui, and Z. Zhong, Phys. Rev. B **102**, 035118 (2020).

65. B. Y. Wang, D. Li, B. H. Goodge, K. Lee, M. Osada, S. P. Harvey, L. F. Kourkoutis, M. R. Beasley, and H. Y. Hwang, Nature Phys. (2021), https://doi.org/10.1038/s41567-020-01128-5, arXiv: 2012.06560.

66. A. S. Botana, V. Pardo, and M. R. Norman, Phys. Rev. Mater. **1**, 021801 (2017).

67. J. Zhang, A. S. Botana, J. W. Freeland, D. Phelan, H. Zheng, V. Pardo, M. R. Norman, and J. F. Mitchell, Nature Phys. **13**, 864 (2017).

68. V. V. Poltavets, K. A. Lokshin, M. Croft, T. K. Mandal, T. Egami, and M. Greenblatt, Inorg. Chem. **46**, 10887 (2007).

69. V. V. Poltavets, K. A. Lokshin, S. Dikmen, M. Croft, T. Egami, and M. Greenblatt, J. Amer. Chem. Soc. **128**, 9050 (2006).

70. V. V. Poltavets, M. Greenblatt, G. H. Fecher, and C. Felser, Phys. Rev. Lett. **102**, 046405 (2009).

71. V. V. Poltavets, K. A. Lokshin, A. H. Nevidomskyy, M. Croft, T. A. Tyson, J. Hadermann, G. Van Tendeloo, T. Egami, G. Kotliar, N. Aproberts-Warren, A. P. Dioguardi, N. J. Curro, and M. Greenblatt, Phys. Rev. Lett. **104**, 206403 (2010).

72. J. Gawraczyński, D. Kurzydłowski, R. A. Ewings, S. Bandaru, W. Gadomski, Z. Mazej, G. Ruani, I. Bergenti, T. Jaroń, A. Ozarowski, S. Hill, P. J. Leszczyński, K. Tokár, M. Derzsi, P. Barone, K. Wohlfeld, J. Lorenzana, and W. Grochala, Proc. Nat. Acad. Sci. **116**, 1495 (2019).

73. M. Hirayama, T. Tadano, Y. Nomura, and R. Arita, Phys. Rev. B **101**, 075107 (2020).

74. F. Bernardini, V. Olevano, X. Blase, and A. Cano, J. Phys. Mater. **3**, 035003 (2020).

75. Z. Z. MG Greenblatt and M. Whangbo, Synth. Met. **85**, 1451 (1997).

76. M. Greenblatt, Curr. Opin. Solid State Mater. Sci. **2**, 174 (1997).

77. J. Karp, A. Hampel, M. Zingl, A. S. Botana, H. Park, M. R. Norman, and A. J. Millis, Phys. Rev. B **102**, 245130 (2020).

78. Z. Li, W. Guo, T. T. Zhang, J. H. Song, T. Y. Gao, Z. B. Gu, and Y. F. Nie, APL Mater. **8**, 091112 (2020).